An experimental and modeling study of HCCI combustion using n-heptane

Guo, Hongsheng; Neill, W. Stuart; Chippior, Wally; Li, Hailin; Taylor, Joshua D.

Publisher's version / Version de l'éditeur:
https://doi.org/10.1115/1.3124667
Journal of Engineering for Gas Turbines and Power, 132, 2, pp. 022801-1-022801-10, 2010-02-01

An Experimental and Modeling Study of HCCI Combustion Using *n*-Heptane

Hongsheng Guo
W. Stuart Neill
Wally Chippior
National Research Council Canada,
1200 Montreal Road,
Ottawa, ON, K1A 0R6, Canada

Hailin Li
West Virginia University,
P.O. Box 6106,
Morgantown, WV, 26506

Joshua D. Taylor
National Renewable Energy Laboratory,
1617 Cole Boulevard,
Golden, CO 80401

Homogeneous charge compression ignition (HCCI) is an advanced low-temperature combustion technology being considered for internal combustion engines due to its potential for high fuel conversion efficiency and extremely low emissions of particulate matter and oxides of nitrogen (NO_x). In its simplest form, HCCI combustion involves the auto-ignition of a homogeneous mixture of fuel, air, and diluents at low to moderate temperatures and high pressure. Previous research has indicated that fuel chemistry has a strong impact on HCCI combustion. This paper reports the preliminary results of an experimental and modeling study of HCCI combustion using n-heptane, a volatile hydrocarbon with well known fuel chemistry. A Co-operative Fuel Research (CFR) engine was modified by the addition of a port fuel injection system to produce a homogeneous fuel-air mixture in the intake manifold, which contributed to a stable and repeatable HCCI combustion process. Detailed experiments were performed to explore the effects of critical engine parameters such as intake temperature, compression ratio, air/fuel ratio, engine speed, turbocharging, and intake mixture throttling on HCCI combustion. The influence of these parameters on the phasing of the low-temperature reaction, main combustion stage, and negative temperature coefficient delay period are presented and discussed. A single-zone numerical simulation with detailed fuel chemistry was developed and validated. The simulations show good agreement with the experimental data and capture important combustion phase trends as engine parameters are varied.
[DOI: 10.1115/1.3124667]

1 Introduction

Homogeneous charge compression ignition (HCCI) is an advanced low-temperature combustion technology. In principle, HCCI involves the auto-ignition of a homogeneous mixture of fuel, air, and diluents at low to moderate temperatures and high pressure. This approach enables the engine designer to have a high compression ratio (CR), minimize air throttling losses, and rapidly burn the fuel-air mixture near top dead center, which contributes to high thermal efficiency. Meanwhile, the burning of a homogeneous fuel-lean mixture at relatively low-temperature suppresses the formation of particulate matter (PM) and oxides of nitrogen (NO_x), the two problematic emissions from diesel engines. These desirable combustion characteristics make HCCI a potentially promising combustion mode for internal combustion engines [1,2].

HCCI was identified as a distinct combustion phenomenon in the late 1970s. Early research [3–5] investigated the potential benefits of HCCI combustion and recognized its potentially attractive characteristics for internal combustion engines. Different approaches for controlling HCCI combustion phasing have been reported [1,5–7]. Christensen et al. [8] demonstrated that HCCI combustion has a multifuel capability compared to traditional internal combustion engines. Recent experimental data available in the open literature [8–12] indicate that fuel chemistry has a strong impact on HCCI combustion. It has been recognized that there is a potential benefit to better understand the fundamentals of HCCI combustion, and, in particular, tailoring a fuel specifically for HCCI combustion [9]. HCCI combustion of both gasoline- and diesel-like fuels and their mixtures has been investigated [10–12]. In these studies, direct injection (DI) diesel engines were adopted due to the increasing interest in employing low-temperature combustion strategies for the reduction in diesel engine emissions [11]. A low-pressure port fuel injector was used in one study to atomize diesel fuels for HCCI combustion research [12].

Apart from fuel chemistry, the fuel injection system and the physical properties of the fuel affect the formation of a homogeneous fuel-air mixture and the HCCI combustion process [11,13]. The experimental results from prototype production engines, typically employing direct injection strategies, reflect the combined effects of fuel injection, fuel-air mixing, and fuel chemistry. The results obtained by different manufacturers may not be consistent due to different fuel injection hardware and combustion strategies adopted to form the homogeneous mixture and control HCCI combustion. This makes it very difficult to ascertain the fuel chemistry effects. In addition, it is very difficult to interpret some experimental data available in the open literature without detailed knowledge of the specific engine hardware and the low-temperature combustion strategy employed. However, detailed information is not always provided, particularly when economic considerations are paramount. Thus, there appears to be a need to develop a method that can be used to evaluate the low-temperature combustion of candidate HCCI fuels, while isolating the effects of the fuel injection system and fuel physical properties.

An engine research facility was constructed to focus on the fuel chemistry aspects of HCCI combustion. The effects of fuel physical properties and fuel system hardware on HCCI combustion were isolated through the adoption of an air-assist port fuel injection system. The system is able to finely atomize a variety of hydrocarbon fuels, leading to a homogeneous air/fuel mixture in the combustion chamber before significant oxidation reactions occur [10,13]. *N*-heptane, a liquid reference fuel with a low boiling point and well known chemistry was used in the current research.

Contributed by the Internal Combustion Engine Division of ASME for publication in the Journal of Engineering for Gas Turbines and Power. Manuscript received November 28, 2006; final manuscript received August 7, 2008; published online October 15, 2009. Review conducted by Christopher J. Rutland. Paper presented at the 2006 Fall Conference of the ASME Internal Combustion Engine Division (ICEF2006), Sacramento, CA, November 5–8, 2006.

Table 1 Engine specifications

Cylinder bore	82.55 mm
Stroke	114.3 mm
Displacement	611.7 ml
Connecting rod length	254 mm
Compression ratio	4.6–16
Combustion chamber	Pancake shape
Intake valve open	10°CA ATDC
Intake valve close	36°CA ABDC
Exhaust valve open	40°CA BBDC
Exhaust valve close	5°CA ATDC
Fuel system	Air-assist port fuel injection

Preliminary research has been conducted to demonstrate its capability to produce stable and repeatable HCCI combustion. In the future, this facility will be used to better understand the role of fuel chemistry in low-temperature combustion and to develop an appropriate method for rating the suitability of HCCI fuels.

Numerical simulations have been widely used to explore fuel chemistry effects on the performance of HCCI engines. Considering the relatively minor influence of physical effects such as turbulence and mixing on HCCI combustion as reported in the literature [1], single- and multizone simulations are suitable tools for exploring fuel chemistry effects on HCCI combustion [14–17], as well as to validate detailed chemical kinetic models [15]. For the current application to predict HCCI combustion phasing, there does not seem to be a requirement to develop a detailed computational fluid dynamics (CFD) model. Also, the large computational requirement for a CFD model limits the ability to implement detailed fuel chemistry, which has been demonstrated to be a critical element in HCCI research [14,15]. Of course, CFD is a useful tool for understanding engine performance and emissions, where the presence of boundary layer and crevices are of great importance.

This paper reports the preliminary results of an experimental and modeling study of HCCI combustion over a wide range of operating conditions using *n*-heptane. The experiments were designed to investigate the effects of a number of engine parameters on the combustion phasing of the low-temperature reaction (LTR) and main combustion stage (MCS), as well as to measure the negative temperature coefficient (NTC) delay period. A numerical model with detailed fuel chemistry was developed and compared to the combustion data obtained in this study. The numerical simulation was able to capture the combustion phasing trends observed during the experiments with changes in several engine parameters. Based on the experimental and numerical results, it is believed that the research engine used in this study is suitable for investigating fuel chemistry effects on HCCI combustion. In the future, the research engine will be used to evaluate the HCCI combustion behavior of real hydrocarbon fuels.

2 Experimental Apparatus and Procedure

2.1 CFR Engine. A Co-operative Fuel Research (CFR) engine was used for this research. It is a single-cylinder, variable compression ratio, four-stroke engine commonly used to evaluate the knock resistance of gasoline and the ignition quality of diesel fuels. Table 1 provides the basic specifications of the CFR engine. Figure 1 shows the schematic of the research facility.

The engine was modified from the standard ASTM setup by the addition of an air-assist port fuel injection system and other hardware and software needed for the control of critical engine parameters such as intake air temperature, air/fuel ratio (AFR), exhaust gas recirculation, and intake and exhaust back pressure.

2.2 Fuel Injection. A port fuel injector for flexible fuel vehicles was modified to provide air-assist atomization of liquid fuels. For this study, the fuel system and air-assist pressures were

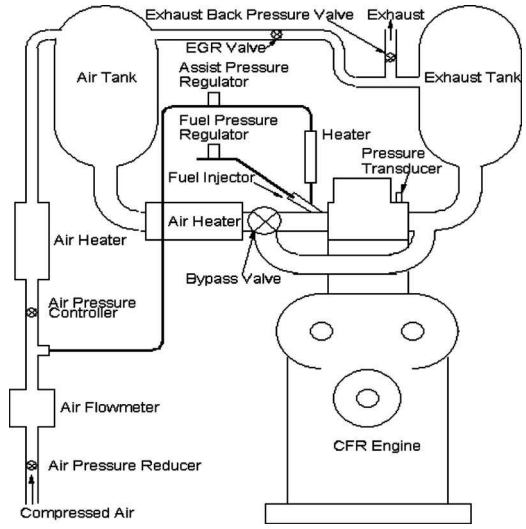

Fig. 1 Schematic of HCCI engine setup

maintained at 500 kPa and 200 kPa, respectively. The injector produces droplets with a Sauter mean diameter (SMD) of 15 μm or less with both diesel- and gasolinelike fuels under these conditions. In this research, the fuel was injected into the intake manifold during the intake stroke. A Coriolis-effect mass flow meter (Micro Motion, Model D6) was used to measure the fuel flow rate. The amount of fuel injected was controlled by adjusting the fuel injection pulse width, and feedback control was provided based on the measured fuel and air flow rates.

2.3 Intake Air and Exhaust Systems. Surge tanks were installed in the intake and exhaust systems to minimize pressure pulsations of the intake and exhaust gases, thereby improving engine operational stability and airflow measurement. The intake air was maintained at a specified temperature by precisely controlling the power supplied to a 1.5 kW heater installed after the intake surge tank. Combustion air was supplied by regulated compressed air and mixed with the desired quantity of recirculated exhaust in the intake surge tank.

The exhaust surge tank provides complete mixing of the exhaust gases before sampling for emissions analysis and recirculation into the intake manifold. A back pressure valve was installed at the exit of exhaust surge tank to create the pressure drop needed for exhaust gas recirculation (EGR) operation and to simulate the back pressure of the turbocharged engine.

The total air flow rate to the engine was measured using a mass flow meter (Sierra, model 780 Series Flat-Trak™). A portion of the air was diverted to assist in fuel atomization prior to entering the intake manifold.

2.4 Data Acquisition. The low-speed data acquisition system is based on National Instruments' PXI hardware platform. The hardware is controlled by data acquisition and control software (Sakor Technologies, Inc., DynoLAB™ PT), which provided stable control of the engine speed and load conditions, as well as critical parameters such as engine coolant and lubricating oil temperatures, intake air pressure and temperature, exhaust back pressure, fuel injection timing, and the quantity of fuel injected.

Cylinder pressure was measured with a high frequency-response piezoelectric pressure transducer (Kistler Corp., model 6121) mounted flush with the cylinder surface using the detonation transducer access port. The transducer was connected to a dual mode charge amplifier (Kistler, model 5010). An encoder fitted to the cam shaft provided a transistor-transistor logic (TTL) signal with a resolution of 0.1 deg camshaft (0.2 deg crankshaft), which was used as the data acquisition clocking pulses to acquire the pressure data and which served also as an input to the fuel and

blast air injection controlling hardware/software. The resultant pressure and crank angle signals were routed to a high-speed data acquisition system (Op-timum Power Technology, model PTrAc), also based on National Instruments' hardware.

2.5 Dynamometer. The engine was coupled to an eddy current dynamometer that absorbed engine load. A variable-speed ac motor, coupled to the dynamometer with an overdrive clutch, was used to start and motor the engine before stable HCCI combustion was initiated, as well as to maintain engine speed when HCCI combustion was unstable.

2.6 Experimental Procedure. Prior to each experiment, the lubricating oil and coolant systems were preheated by electric heaters to a temperature of 82°C. At the same time, the intake and exhaust systems were also preheated. HCCI combustion was easily initiated after the coolant, lubricating oil, and fuel/air mixture temperatures reached the desired levels. At each operating condition, the engine was run for at least 5 min or until engine operation stabilized before sampling experimental data while continually monitoring key operating parameters such as intake pressure and temperature, as well as brake power, brake specific fuel consumption (BSFC) and unburned hydrocarbon (UHC) and carbon monoxide (CO) emissions.

At each operating condition, engine performance data and critical operating parameters were collected for approximately 4 min at a sampling frequency of 1 Hz. At the same time, 500 engine working cycles were sampled, stored, and processed. The averaged cylinder pressure was analyzed to obtain the heat release and a complete set of combustion parameters such as CA50 and NTC delay period. Each cycle was analyzed individually and used to calculate statistical results such as the COV_{IMEP}. In this research, pure *n*-heptane was used as fuel.

3 Numerical Simulation

In order to predict the combustion process of the HCCI engine, a numerical model with detailed chemistry was developed to simulate the four-stroke process. The intake stroke was simulated while accounting for the presence of residual gases and fresh charge efficiency measured experimentally. The air-fuel-diluents mixture was assumed to be an ideal gas with uniform temperature, pressure, and mixture composition. If blow-by is neglected, the energy conservation equation for the working fluid at any instant in time t, from intake valve closure to exhaust valve opening, is

$$\frac{dQ}{dt} = \frac{dU}{dt} + \frac{dW}{dt} \tag{1}$$

where Q is the heat transfer to the cylinder charge, U is the total internal energy of the cylinder charge, and W is work output due to piston movement.

dW/dt is given by

$$\frac{dW}{dt} = P\frac{dV}{dt} \tag{2}$$

where P is the cylinder pressure, and V is the volume of the combustion chamber.

dQ/dt is given by

$$\frac{dQ}{dt} = -h \cdot A(T - T_w) \tag{3}$$

where A is the surface area of the combustion chamber wall, T is the mean temperature of the charge, T_w is the cylinder wall temperature that is assumed to be constant throughout the cycle, and h is the heat transfer coefficient. Traditionally, h is estimated using an empirical equation developed by Woschni [18] and Heywood [19]. The equation was derived for a propagating turbulent flame, which is obviously not the case of HCCI engine. In this research, the heat transfer coefficient was calculated using formulations derived recently by Chang et al. [20] based on spatially averaged heat flux measurements of HCCI combustion using gasoline.

dU/dt may be calculated as

$$\frac{dU}{dt} = \frac{d\sum(N_i u_i)}{dt} = \sum N_i \frac{du_i}{dt} + \sum u_i \frac{dN_i}{dt} \tag{4}$$

where N_i is the number of moles of the ith species. It changes with time as a result of a chemical reaction as follows:

$$\frac{dN_i}{dt} = V\dot{\omega}_i \tag{5}$$

where $\dot{\omega}_i$ is the production rate of the ith species and can be calculated using CHEMKIN subroutines based on the instantaneous mixture composition, temperature, and pressure. The remaining thermodynamic properties such as internal energy and specific heat capacity were also calculated using CHEMKIN with the corresponding species property data reported in the literature [21].

The presence of residual gases was also considered. The temperature and composition of the combustion products at the exhaust valve closing of the prior engine cycle was used to calculate the residual gas composition and other properties such as enthalpy of the bulk mixture of the following cycle. After adjusting the temperature and composition of the calculated residual gases, the cycle calculation was repeated until the cylinder mixture temperature from one cycle to the next varied by less than 0.5°C at the exhaust valve opening. Under normal conditions, the cylinder mixture temperature converged after three engine cycles. When the combustion process was retarded, however, it took more than five cycles to obtain a stable exhaust temperature considering the significant effect of intake temperature on HCCI combustion under such conditions.

3.1 Effective Fuel/Air Mixture Temperature. In this research, the intake air-diluent mixture temperature was measured using a thermocouple installed about 25 cm upstream of the intake valve and 5 cm upstream of fuel injector. However, the intake mixture is cooled due to fuel evaporation and then continually heated by the intake port and intake valve. Accordingly, the effective fuel/air mixture temperature entering the combustion chamber must be estimated. Following the procedure recommended in literature [22], the effective intake temperature $T_{\text{in,effective}}$ was estimated as follows:

$$T_{\text{in,effective}} = T_{\text{in,effective,base}} \cdot \frac{\dot{m}_{\text{air,base}}}{\dot{m}_{\text{air+fuel}}} \cdot \frac{M_{\text{air+fuel}}}{M_{\text{air}}} \cdot \frac{P_{\text{in}}}{P_{\text{in,base}}} \tag{6}$$

where $\dot{m}_{\text{air+fuel}}$, $M_{\text{air+fuel}}$, and P_{in} are the mass flow rate, molar mass, and pressure of intake mixture, respectively; $\dot{m}_{\text{air,base}}$, $M_{\text{air,base}}$, and $P_{\text{in,base}}$ are the mass flow rate, molar mass, and intake air pressure for the base case, respectively; and $T_{\text{in,effective,base}}$ is the effective intake temperature for the base case.

In principle, the base case can be any experimental condition for which the effective intake temperature can be accurately estimated or computed. For this study, the base case involved motoring the engine at a constant speed while maintaining the intake air and lubricating oil and coolant temperatures at 82°C. Under these conditions, heat transfer between the intake mixture and the intake port and valve is minimized and the effective fuel/air mixture temperature will be close to the intake air temperature. Figure 2 shows the variation of the effective intake mixture temperature as a function of the intake air temperature with a constant AFR. For 20°C intake air temperature, the effective intake mixture temperature was about 20°C higher than the measured intake air temperature. The effective intake mixture temperature was equivalent to the intake air temperature with an intake air temperature of 82°C, as shown in Fig. 2.

3.2 Fuel Chemistry. A detailed chemistry, consisted of 561 species and 2539 elementary reactions, was adopted to simulate the ignition process for *n*-haptane-air mixtures [21]. This is the

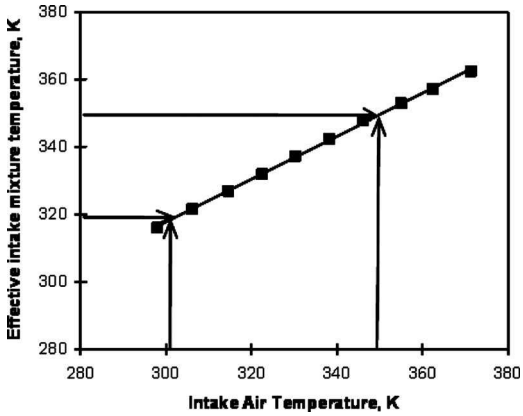

Fig. 2 Variation of effective intake mixture temperature with intake air temperature: N=900 rpm, CR=10.0, P_{in}=95 kPa, P_{exh}=104 kPa, AFR=50

most detailed chemistry for n-heptane [15,21] and has been shown to be suitable for HCCI engine simulations using a single-zone model [15].

3.3 Validation of Numerical Simulation. The aforementioned numerical simulation with detailed fuel chemistry was first validated against shock tube data reported in the literature [21,23]. As shown in Fig. 3, the ignition delay calculated by the model agrees well with experimental data measured under both stoichiometric and lean conditions over a range of temperatures and pressures [21,23]. This confirms that the chemistry scheme employed can simulate the n-heptane oxidation process and predict the ignition delay measured in a shock tube. Accordingly, this chemistry was used in this research to examine HCCI combustion. As an example, the predicted results were also compared to pressure traces generated by CHEMKIN IV, a well known commercial software package, for adiabatic HCCI combustion. The model developed produced identical cylinder pressure and temperature traces to those generated by CHEMKIN IV when heat transfer between bulk gas and engine coolant was neglected. This confirms that the numerical simulation can be used to calculate the combustion process of HCCI engine if a suitable heat transfer equation is employed.

4 Results and Discussion

Figure 4 shows a typical HCCI combustion trace using n-heptane. The motoring cylinder pressure is shown for comparison purposes. As reported by many other researchers, n-heptane

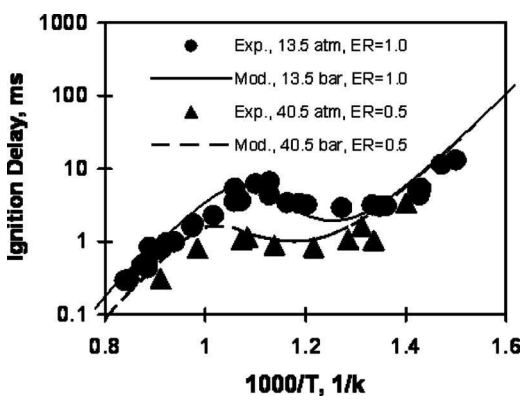

Fig. 3 Ignition delay of n-heptane at moderate and high pressure for both lean and stoichiometric mixtures. Experimental data were obtained from Ref. [23].

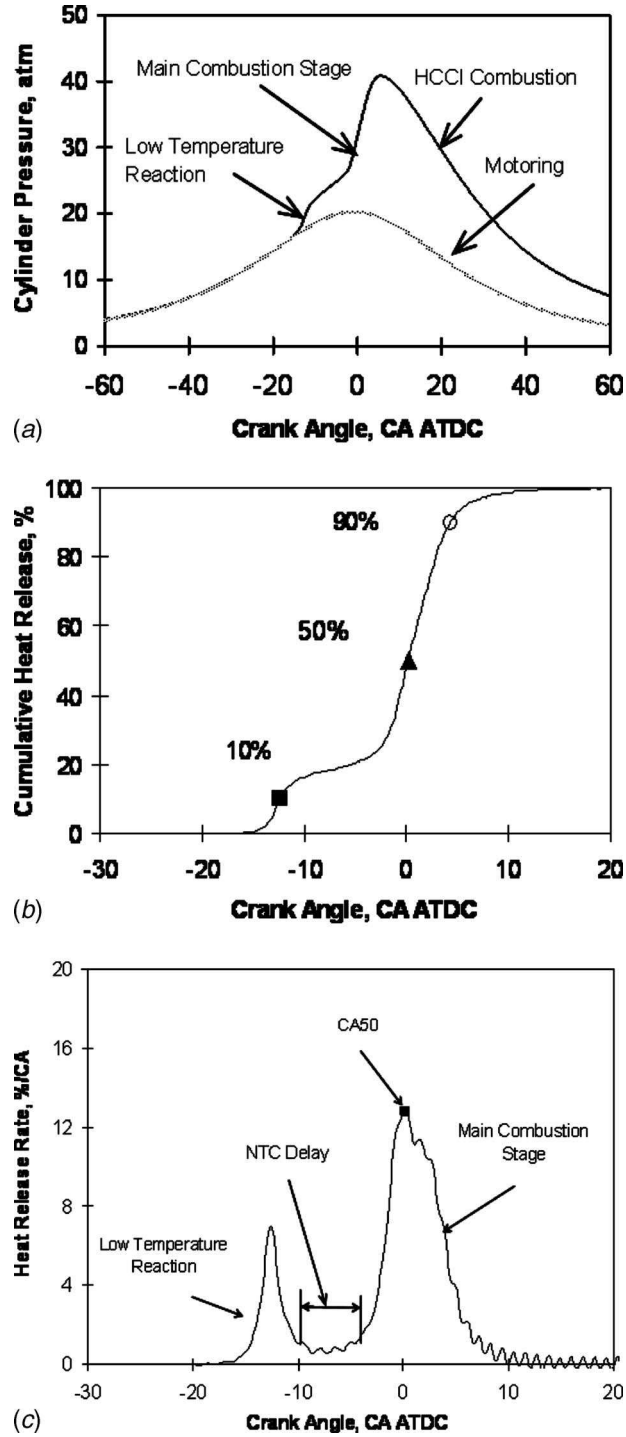

Fig. 4 Variation of (a) cylinder pressure (HCCI and motoring), (b) cumulative heat release, and (c) heat release rate with crank angle; CR=10, T_{in}=30°C, AFR=50, P_{in}=95 kPa

combustion is characterized by a well known two-stage oxidation process. The first stage is associated with LTRs and releases a relatively small amount of energy. The second stage associated with high temperature oxidation releases most of the energy and is considered as the MCS. In this research, the crank angle duration between the end of the LTR and the beginning of the MCS is defined as the NTC delay, as shown in Fig. 4(c). The heat release process was characterized by the start (10% heat release, CA10), middle (50%, CA50), and end (90%, CA90) of combustion as shown in Fig. 4(b). The location of 50% heat release (CA50) is

Table 2 Repeatability of HCCI engine operation (CR=10.0, T_{in} =30°C, P_{in}=95 kPa, P_{exh}=104 kPa, AFR=50)

Test No.	CA10[a]	CA50[a]	CA90[a]	IMEP (bar)	COV_{IMEP} (%)	ISFC (g/kW h)
1	−11.72	0.20	2.80	3.42	2.3	213.1
2	−12.53	0.68	5.47	3.28	2.0	221.6
3	−12.41	0.24	4.42	3.34	2.0	215.2
4	−12.53	−0.33	3.45	3.41	2.2	213. 6

[a]°CA ATDC.

generally considered to be the most important parameter that is adjusted to optimize HCCI combustion phasing. As shown in Fig. 4(*c*), CA50 is located close to the middle of the main combustion stage. For this condition, the engine produced near-zero soot emissions measured by laser-induced incandescence (Artium Technologies) and less than 2 ppm NO_x emissions (California Analytical Instruments), reflecting excellent HCCI combustion [24].

Table 2 compares the combustion process, indicated engine performance and combustion stability obtained in a series of experiments conducted over a 2 week period under the prescribed operating conditions. The data show that stable and repeatable HCCI combustion has been achieved at this operating condition. For example, the observed differences in CA10 and CA50 were within 1°CA and the coefficient of variation (COV) in the indicated mean effective pressure (IMEP) was found to be about 2%.

On the basis of these preliminary results, the experimental apparatus was used to investigate the effects of critical engine parameters on HCCI combustion. Details of the experimental matrix are provided in Table 3. The experimental results are shown in Figs. 5–11.

Figure 5 shows the effect of engine speed on HCCI combustion. Increasing engine speed tends to reduce cylinder pressure and retard the peak pressure location as shown in Fig. 5(*a*). This is due to a significantly retarded MCS, as shown in Fig. 5(*b*). The heat release rate during the MCS is also reduced with retarded combustion due to the increasing combustion chamber volume after top dead center. This leads to lower combustion chamber temperatures and a corresponding decrease in the oxidation reaction rates. However, the effect of engine speed on the LTR phase tends to be relatively weak, reflecting its strong dependence on temperature history. Increasing the engine speed delays the phasing of the MCS, primarily due to its effect on the NTC delay period. Figure 6 shows that the NTC delay increases linearly with increasing engine speed, reflecting the constant NTC delay period (in seconds) under constant AFR conditions.

Similar to spark ignition and diesel engines, the work produced by an HCCI engine is controlled by adjusting the amount of fuel supplied. Figure 7 shows the effect of AFR on cylinder pressure and heat release rate when intake air temperature was kept constant. As shown in Fig. 7(*a*), the cylinder pressure increases more rapidly and reaches its peak value at an earlier crank angle when the fueling rate is increased, which corresponds to a lower AFR. The advanced MCS combined with the enhanced heat release rate,

Table 3 Experiment matrix

Test No.	Speed (rpm)	AFR (mass)	CR	$T_{in,air}$ (°C)	P_{in} (kPa)
1	600–1400	50	10.0	40	95
2	900	43–63	10.0	40	95
3	900	50	9–16	30	95
4	900	50, 60	10.0	25–100	95
5	900	60	10.0	40	95–200
6[a]	900	20–60	10.0	40	40–95

[a]Constant fuel flow rate.

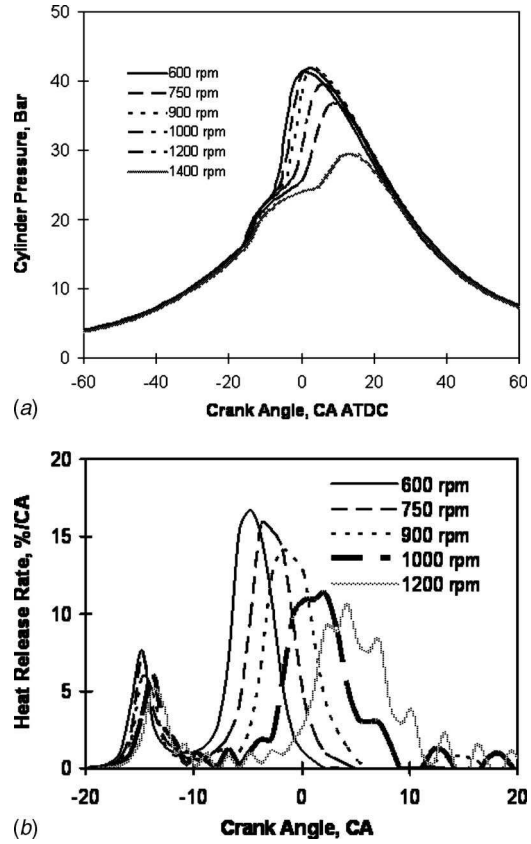

Fig. 5 Effect of engine speed on (*a*) cylinder pressure and (*b*) heat release rate: CR=10.0, AFR=50, $T_{in,air}$=40°C, P_{in}=95 kPa, P_{exh}=104 kPa

as shown in Fig. 7(*b*), contributes to this phenomenon. Similar to the effect of engine speed, AFR does not have a large influence on the phasing of the LTR, indicating a stronger dependence on mixture temperature history than on mixture composition. In comparison, increasing the AFR by reducing the fueling rate significantly retarded the phasing of the MCS. This is primarily due to the effect of leaner conditions on the NTC delay period, as shown in Fig. 8. The NTC delay increases almost linearly with increasing AFR.

The effect of turbocharging on HCCI combustion was examined at a constant AFR condition. As shown in Fig. 9, boosting the

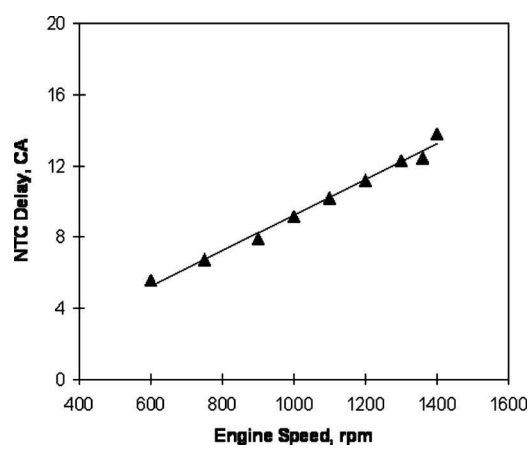

Fig. 6 Effect of engine speed on NTC delay: CR=10.0, $T_{in,air}$ =40°C, P_{in}=95 kPa, P_{exh}=104 kPa, fuel: *n*-heptane, AFR=50.

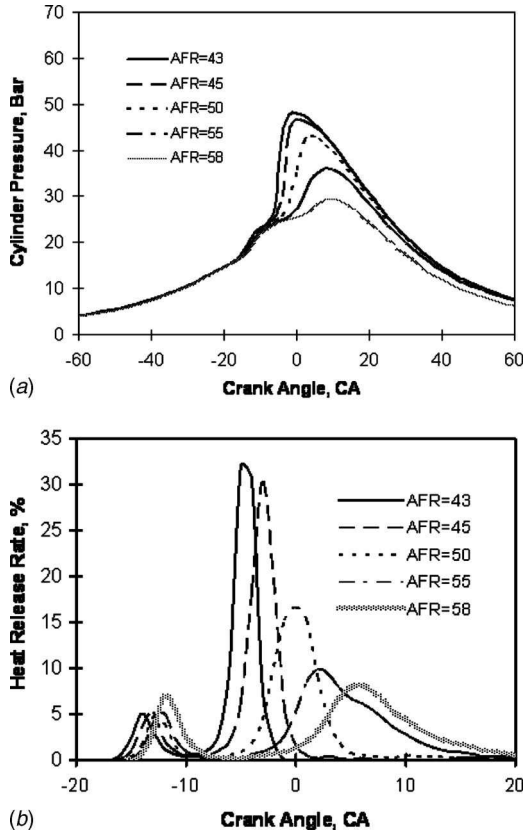

Fig. 7 (*a*) **Cylinder pressure;** (*b*) **heat release rate. Effect of air-fuel ratio on HCCI combustion: CR=10.0,** $T_{in,air}$**=40°C,** P_{in} **=95 kPa,** P_{exh}**=104 kPa, N=900 rpm.**

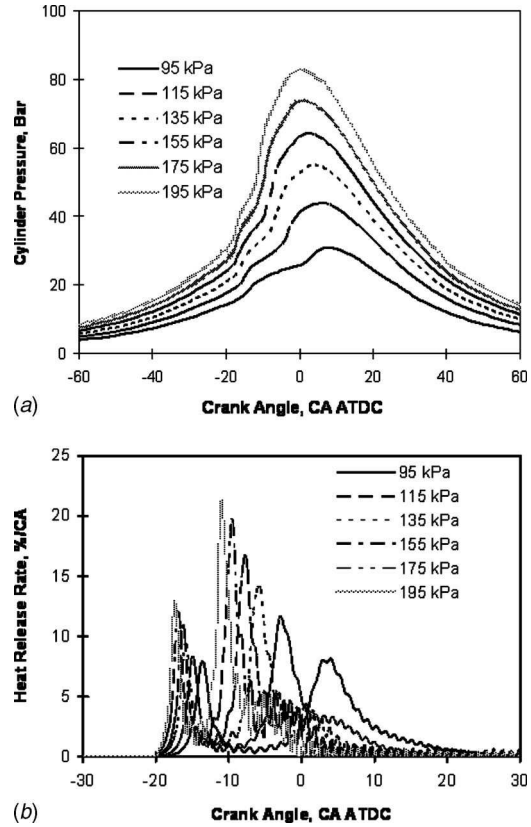

Fig. 9 (*a*) **Cylinder pressure;** (*b*) **heat release rate. Effect of turbocharging on HCCI combustion: CR=10,** $T_{in,air}$**=40°C, AFR =60.0,** N**=900 rpm.**

intake pressure tends to significantly increase the cylinder pressure during the compression stroke. Since the quantity of fuel injected is increased as intake pressure increases to maintain a constant AFR, the LTR stage is advanced and intensified. This leads to a shorter NTC delay period and significantly advances phasing of the MCS, as shown in Fig. 9(*b*). Figure 10 shows that increasing the intake pressure significantly reduces the NTC delay period as the intake pressure is increased from 80 kPa to 120 kPa. Boosting the intake pressure beyond 120 kPa continued to reduce the NTC delay period, but the rate of decrease in the NTC delay period was lower.

Intake temperature is the most critical and widely used engine operation parameter to control the phasing of HCCI combustion. Figure 11 shows the effect of intake temperature on HCCI combustion for a constant AFR of 50. Stable HCCI combustion was obtained for a wide range of temperatures. As shown in Fig. 11(*b*), increasing the intake temperature advances the phasing of both the LTR and MCS. The LTR heat release profiles were found to be quite similar, although they were advanced as temperature increased. However, increasing the intake temperature significantly enhances the heat release rate of the MCS. The increasingly advanced phasing of the MCS contributes to the increased heat release rate. As shown in Fig. 12, intake temperature does not have a large influence on the NTC delay period.

Figure 13 shows that increasing the compression ratio advances the combustion process and increases the peak cylinder pressures.

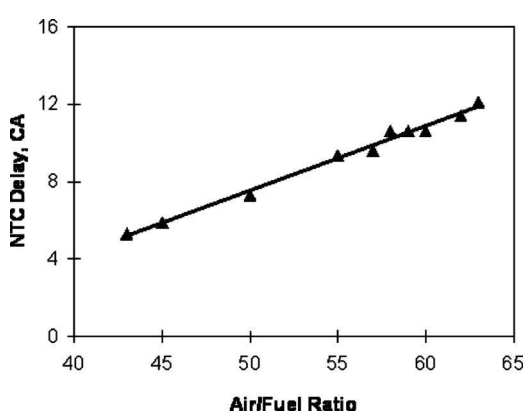

Fig. 8 Effect of air-fuel ratio on NTC delay: CR=10.0, $T_{in,air}$ **=40°C,** P_{in}**=95 kPa,** P_{exh}**=104 kPa,** N**=900 rpm**

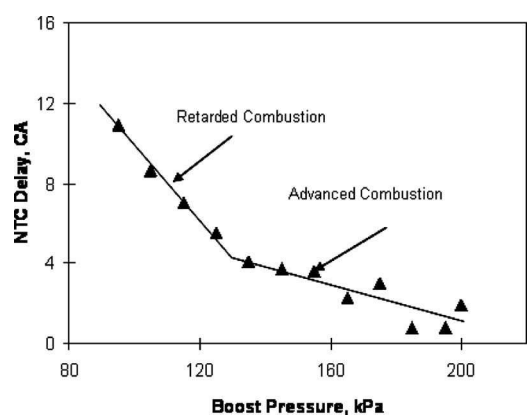

Fig. 10 Effect of turbocharging on NTC delay: CR=10, $T_{in,air}$ **=40°C, AFR=60.0,** N**=900 rpm**

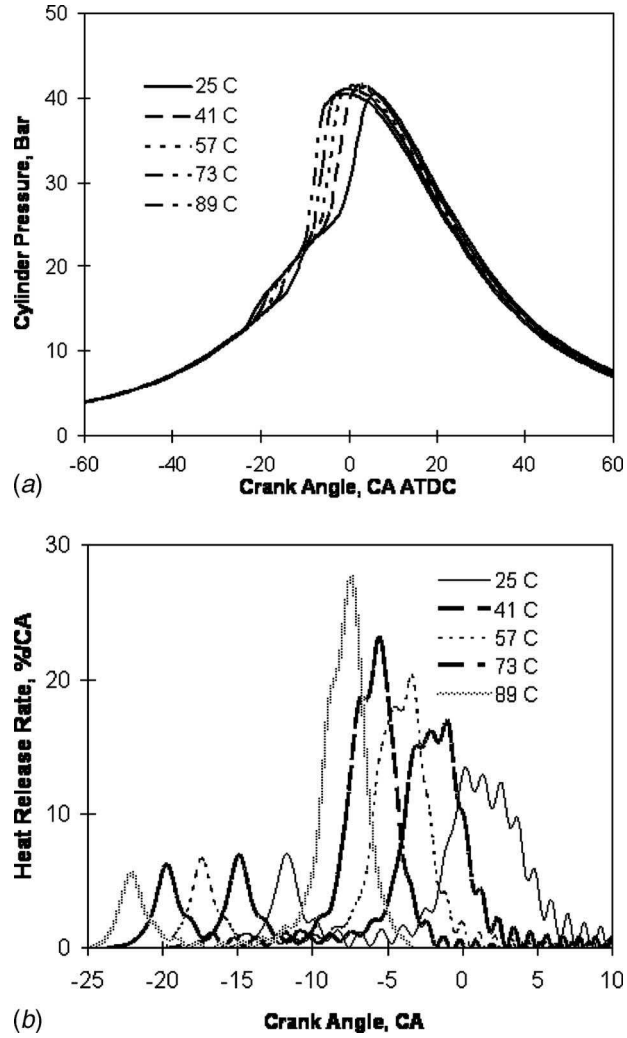

Fig. 11 (*a*) Cylinder pressure; (*b*) heat release rate. Effect of intake air temperature on HCCI combustion: N=900 rpm, CR =10.0, P_{in}=95 kPa, P_{exh}=104 kPa, AFR=50.

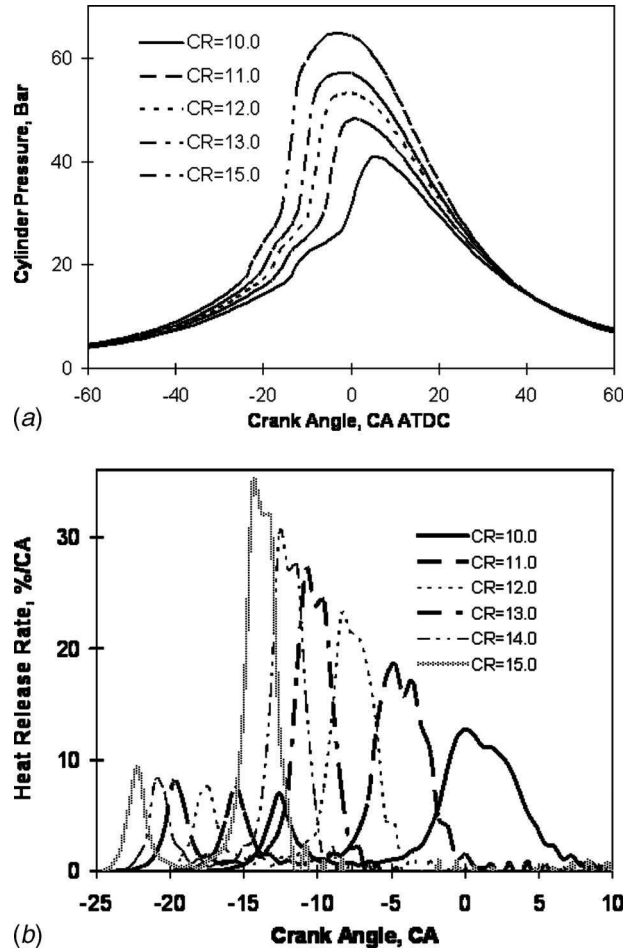

Fig. 13 (*a*) Cylinder pressure; (*b*) heat release rate. Effect of compression ratio on HCCI combustion: $T_{in,air}$=30°C, P_{in} =95 kPa, P_{exh}=104 kPa, N=900 rpm, AFR=50.

This is primarily due to the effect of increased compression temperatures and pressures as the compression ratio increases, which enhances *n*-heptane oxidation. As shown in Fig. 13(*b*), the phasing of both LTR and MCS phases were advanced with increasing compression ratio. Figure 14 shows that increasing the compression ratio from 9 to 10 dramatically decreased the NTC delay period. For a compression ratio of 11, the MCS was advanced beyond top dead center. Increasing the compression ratio beyond 11 had a negligible effect on the NTC delay period. The combustion phasing of the LTR and MSC were advanced by a comparable amount as compression ratio was increased beyond 11.

HCCI combustion tends to become unstable and incomplete when the MCS is retarded excessively. In these cases, the combustion phasing can be advanced by heating the intake mixture to a higher temperature or increasing the compression ratio. As re-

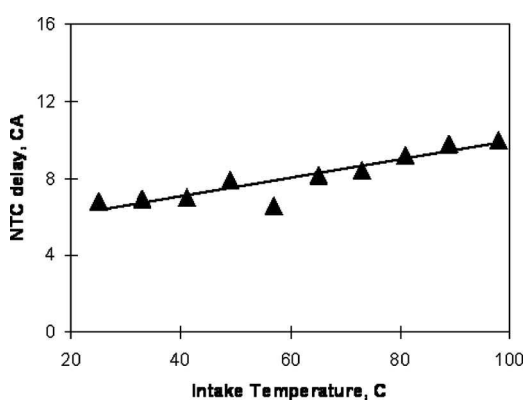

Fig. 12 Effect of intake air temperature on NTC delay: N =900 rpm, CR=10.0, P_{in}=95 kPa, P_{exh}=104 kPa, AFR=50

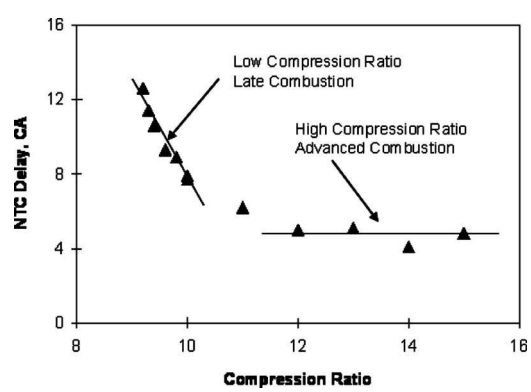

Fig. 14 Effect of compression ratio on NTC delay: $T_{in,air}$ =30°C, P_{in}=95 kPa, P_{exh}=104 kPa, N=900 rpm, AFR=50

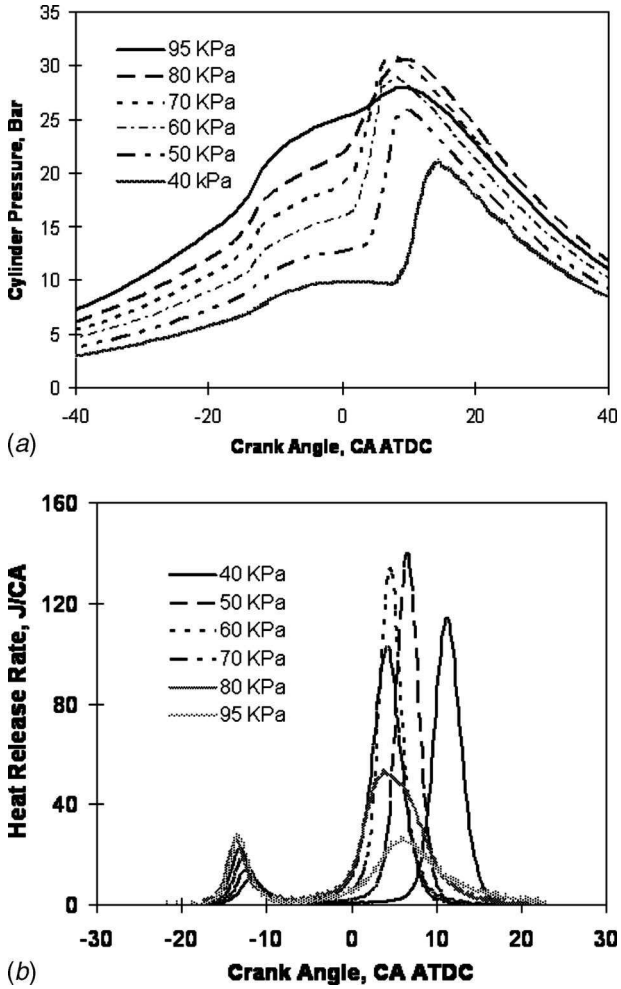

Fig. 15 (*a*) Cylinder pressure; (*b*) heat release rate. Effect of intake air throttling on HCCI combustion at constant intake fuel flow rate: N=900 rpm, CR=10.0, $T_{in,air}$=40°C, P_{exh}=104 kPa, $\dot{m}_{fuel}$=0.273 kg/h, AFR=20–60.

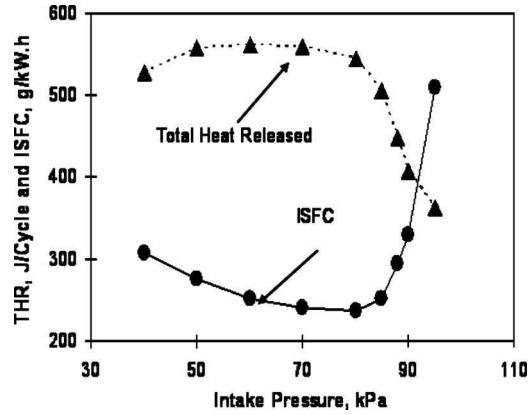

Fig. 16 Effect of throttling intake air on total heat release and indicated specific fuel consumption when intake fuel flow rate was kept constant: N=900 rpm, CR=10.0, $T_{in,air}$=40°C, P_{exh}=104 kPa, $\dot{m}_{fuel}$=0.273 kg/h, AFR=20–60

ported in the literature [25], enriching the air/fuel mixture under lean operation can enhance the oxidation reaction rates. The experiments that examined AFR effects on HCCI combustion in this study demonstrated that a relatively richer mixture helps to advance the combustion phase and accelerate the oxidation process to achieve complete combustion. Traditionally, enriching the intake mixture is achieved by injecting more fuel into the intake air. However, this same effect may also be obtained by throttling the intake air while keeping the fuel flow rate constant. Figure 15 shows the effect of intake air throttling on HCCI combustion under a constant fuel flow rate condition. Late and incomplete combustion was encountered with 95 kPa intake pressure, which is reflected by a relatively weak MCS and reduced heat release during the combustion process. Throttling the intake air enhanced the heat release during the MCS, although its effect on the combustion phasing of the LTR is relatively weak, as shown in Fig. 15(*b*). Intake air throttling can help to burn the fuel completely as indicated by the increased total heat release and reduced indicated specific fuel consumption (ISFC), as shown in Fig. 16. Throttling the intake air enables complete combustion even though the MCS occurs after top dead center. The presence of less excess air (a diluent) in the combustion chamber helps to increase the bulk gas temperature and enhance the oxidation process during the MCS. However, overthrottling the intake pressure tends to delay the MCS again. This is due to the effect of cylinder pressure on the combustion process, as well as the increasing role played by residual gases, which tends to deteriorate the oxidation process and retard the main combustion phase [26]. As shown in Fig. 16, ISFC increases when the intake pressure is overthrottled. This is due to increased pumping losses and the reduced oxidation rate associated with having a higher fraction of residual gases.

The aforementioned single-zone numerical model was used to simulate the HCCI combustion process. Figure 17 compares the predicted cylinder pressure, heat release rate, and cumulative heat release with those measured experimentally. For comparison purposes, the effective intake mixture temperature used in the simulation was adjusted such that the calculated CA50 matched experimental data. The effective intake temperature used in the numerical simulation was 350 K compared with the experimental value of 319.5 K as calculated by Eq. (6). Other researchers have reported a need to adjust the intake mixture temperature in modeling HCCI combustion. For example, Yelvington et al. [27] reported that the intake temperature adjustment was approximately 30 K in order to match the predicted phasing of the heat release with experimental data. This is likely due to the imperfect assumption of a homogeneous air/fuel mixture with uniform temperature, pressure, and reaction rate, as well as potential limitations of the fuel chemistry. The assumption of uniform and constant combustion chamber wall temperature during the whole engine cycle may also contribute to the requirement to adjust the intake mixture temperature. Intake mixture temperature adjustments have also been used in multizone models to account for nonuniformities of the mixture temperature. For example, an initial temperature difference between the core and outer boundary zones in one multizone numerical simulation was reported to be ~35 K to achieve reasonable predictions of cylinder pressure and combustion phasing [28,29].

As shown in Fig. 17, the numerical simulation was able to capture elements of HCCI combustion of *n*-heptane, particularly the phasing of the MCS. In comparison, the LTR predicted by the numerical simulation is advanced compared to the experimental data as shown in Figs. 17(*b*) and 17(*c*). A spike in the predicted heat release rate was observed during the MCS. This spike was caused by the rapid oxidation of all CO accumulated to this point in the simulation to CO_2. The conversion of CO to CO_2 is predicted to happen rapidly once the required temperature is reached because only a few reactions are involved. Rapid oxidation of CO to CO_2 has not been observed experimentally or reported in the oliterature. The assumption of uniform mixture temperature and mixture composition contributes to this overly-rapid heat release rate.

For this research, a single adjustment was made to the effective intake mixture temperature and then applied to all operating con-

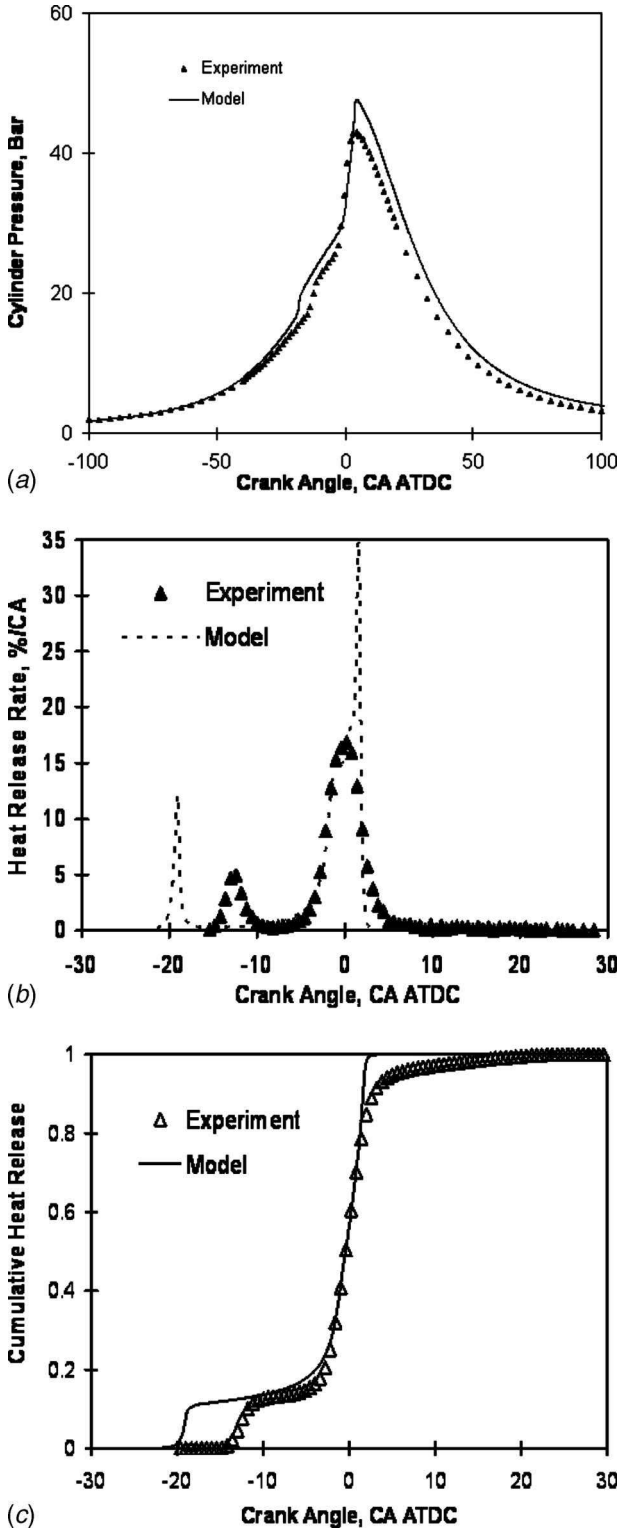

Fig. 17 Comparison of predicted (*a*) cylinder pressure, (*b*) heat release rate, and (c) cumulative heat release with experimental data: CR=10, $T_{in,air}$=30°C, AFR=50, P_{in}=95 kPa

ditions. On this basis, this model was shown to be able to capture the effect of compression ratio on the combustion phasing of HCCI combustion using *n*-heptane. Figure 18 compares the predicted CA50 with those measured experimentally for different compression ratios while keeping the AFR constant at 50. The predicted CA50 combustion phasing was found to agree well with

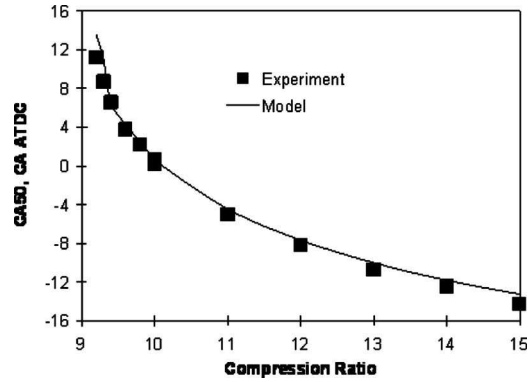

Fig. 18 Comparison of the predicted CA50 with those determined experimentally over a range of compression ratios. Operating condition is the same as Fig. 13.

the experimental measurements. It was found that CA50 retards almost linearly with decreasing CR for high compression ratios (CR > 11). However, the CA50 retards rapidly when the compression ratio is reduced below 10, reflecting an increasing sensitivity for *n*-heptane when CA50 occurs after top dead center.

Figure 19 shows that the numerical simulation is able to capture the approximately linear trend of CA50 retardation as engine speed increases.

Finally, the effect of turbocharging on CA50 may be seen in Fig. 20. For this figure, the effective intake mixture temperature in the numerical simulation was adjusted to match the experimental data when the intake pressure was 95 kPa. Figure 20 shows that the numerical simulation is able to capture the trend of advanced

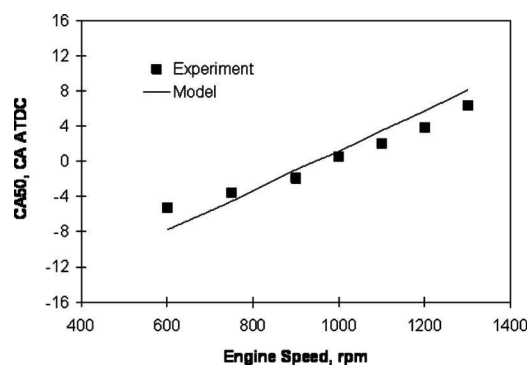

Fig. 19 Comparison of the predicted CA50 with those determined experimentally over a range of engine speeds. Operating condition is the same as in Fig. 5.

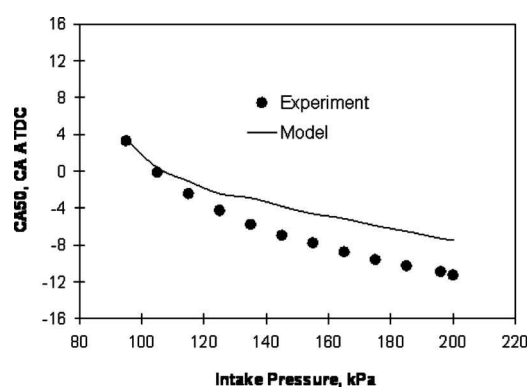

Fig. 20 Comparison of the predicted CA50 with those determined experimentally over a range of intake pressures. Operating condition is the same as in Fig. 9.

CA50 as intake pressure increases. However, the predicted CA50 is retarded relative to the experimental data at higher intake pressures. The assumption that the combustion chamber wall temperature is not a function of engine load may be responsible for this difference. Since the combustion chamber wall temperature likely increases with increasing load, incorporating a variable combustion wall temperature should improve the predictions of CA50 under turbocharged conditions.

5 Conclusions

A CFR engine was modified to investigate HCCI combustion characteristics over a wide range of operating conditions. In particular, a port fuel injection system was implemented for atomizing *n*-heptane for this study. Based on the experimental data and complementary numerical simulations of HCCI combustion, the following conclusions may be drawn.

- Increasing the intake air temperature and compression ratio advances the phasing of both the low-temperature reaction and main combustion stage. In comparison, the effects of AFR, engine speed, and turbocharging on the phasing of low-temperature reaction are relatively weak, but they significantly affect the phasing of the main combustion stage.
- The NTC delay period is a strong function of engine speed, air/fuel ratio, and intake pressure (at constant air/fuel ratio). The effect of intake temperature (at constant air/fuel ratio) on the NTC delay period is not as strong as those previously described. In comparison, the effect of compression ratio on NTC delay is negligible except for low compression ratios when the combustion phasing is very retarded.
- Throttling the intake air while keeping fuel flow rate constant tends to improve HCCI combustion when incomplete combustion is observed. It is believed that the resultant enrichment of the air/fuel mixture contributes to this desirable characteristic. However, overthrottling tends to retard the main combustion stage and deteriorate engine performance even though relatively complete combustion can still be obtained at a later combustion phasing.
- The validated numerical simulation was able to capture trends in combustion phasing variation with critical engine parameters. The calculated CA50 was found to agree well with those measured experimentally over a wide range of engine compression ratios, speeds, and intake pressures.

Acknowledgement

The financial support of the Government of Canada's PERD/AFTER and Climate Change T&II programs are gratefully acknowledged. The technical contribution of Mr. M. F. Baksh in constructing the fuel delivery system is acknowledged.

References

[1] Epping, K., Aceves, S. M., Bechtold, R. L., and Dec, J. E., 2002, "The Potential of HCCI Combustion for High Efficiency and Low Emissions," SAE Paper No. 2002-01-1923.
[2] Zhao, F., Asmus, T, Assanis, D., Dec, J., Eng, J., and Najt, P, 2003, "Homogeneous Charge Compression Ignition (HCCI) Engines: Key Research and Development Issues," Society of Automotive Engineers, Inc., SAE Paper No. PT-94.
[3] Onishi, S., Jo, S. H., Shoda, K., Jo, P. D., and Kato, S., 1979, "Active Thermo-Atmosphere Combustion (ATAC)–A New Combustion Process for Internal Combustion Engines," SAE Paper No. 790501.
[4] Noguchi, M., Tanaka, Y., Tanaka, T., and Takeuchi, Y., 1979, "A Study on Gasoline Engine Combustion by Observation of Intermediate Reactive Products During Combustion," SAE Paper No. 790840.
[5] Najt, P. M., and Foster, D. E., 1983, "Compression-Ignited Homogeneous Charge Combustion," SAE Paper No. 830264.
[6] Chen, R. and Milovanovic, N., 2001, "A Review of Experimental and Simulation Studies on Controlled Auto-Ignition Combustion," SAE Paper No. 2001-01-1890.
[7] Yang, J., Culp, T., and Kenney, T., 2002, "Development of a Gasoline Engine System Using HCCI Technology—The Concept and the Test Results," SAE Paper 2002-01-2832.
[8] Christensen, M., Hultqvist, A., and Johansson, B., 1999, "Demonstrating the Multi-Fuel Capability of a Homogeneous Charge Compression Ignition Engine With Variable Compression Ratio," SAE Paper No. 1999-01-3679.
[9] Kalghatgi, G. T., 2005, "Auto-Ignition Quality of Practical Fuels and Implication for Fuel Requirements of Future SI and HCCI Engines," SAE Paper No. 2005-01-0239.
[10] Amann, M., Ryan, T. W., and Kono, N., 2005, "HCCI Fuels Evaluations-Gasoline Boiling Range Fuels," SAE Paper No. 2005-01-3727.
[11] Ryan, T.W., Callahan, T.J., and Mehta, D., 2004, "HCCI in a Variable Compression Ratio Engine—Effects of Engine Variables," SAE Paper No. 2004-01-1971.
[12] Zhong, S., Megaritis, A., Yap, D., and Xu, H., 2005, "Experimental Investigation Into HCCI Combustion Using Gasoline and Diesel Blended Fuels," SAE Paper No. 2005-01-3733.
[13] Li, Y., Zhao, H., Brouzos, N., Ma, T., and Leach, B., 2006, "Effect of Injection Timing on Mixture and CAI Combustion in a GDI Engine With an Air-Assisted Injector," SAE Paper No. 2006-01-0206.
[14] Easley, W., Agarwal, A., and Lavoie, G. A., 2001, "Modeling of HCCI Combustion and Emissions Using Detailed Chemistry," SAE Paper No. 2001-01-1029.
[15] Naik, C., Pitz, W. J., Sjoberg, M., Dec, J. E., Orme, J., Curran, H., Simmie, J. M., and Westbrook, C. K., 2005, "Detailed Chemical Kinetic Modelling of Surrogate Fuels for Gasoline and Application to an HCCI Engine," SAE Paper No. 2005-01-3741.
[16] Xu, H., 2005, "Modelling of HCCI Engines: Comparison of Single-Zone, Multi-Zone and Test Data," SAE Paper No. 2005-01-2123.
[17] Kongsereeparp, P., Kashani, B., and Checkel, M. D., 2005, "A Stand-Alone Multi-Zone Model for Combustion in HCCI Engines," ASME ICED 2005 Fall Technical Conference, Ottawa, Canada, Sept.11–14, ASME Paper No. ICEF2005-1241.
[18] Woschni, G., 1967, "A Universal Applicable Equation for the Instantaneous Heat Transfer Coefficient in the Internal Combustion Engines," SAE Paper No. 670971.
[19] Heywood, J. B., 1988, *Internal Combustion Engine Fundamentals*, McGraw-Hill, New York.
[20] Chang, J., Guralp, O., Asanis, D., Kuo, T., Najt, P., and Rask, R., 2004, "New Heat Transfer Correlation for an HCCI Engine Derived From Measurements of Instantaneous Surface Heat Flux," SAE Paper No. 2004-01-2996.
[21] Curran, H. J., Gaffuri, P., Pitz, W. J., and Westbrook, C. K., 1998, "A Comprehensive Modeling Study of *n*-Heptane Oxidation," Combust. Flame, **114**, pp. 149–177.
[22] Sjöberg, M., and Dec, J.E., 2004, "An Investigation of the Relationship Between Measured Intake Temperature, BDC Temperature, and Combustion Phasing for Premixed and DI HCCI Engines," SAE Paper No. 2004-01-1900.
[23] Ciezki, H. K., and Adomeit, G., 1993, "Shock-Tube Investigation of Self-Ignition of n-Heptane-Air Mixtures Under Engine Related Conditions," Combust. Flame, **93**, pp. 421–433.
[24] Li, H. L., Neill, W. S., Chippior, W., Graham, L., Connolly, T., and Taylor, J. D., 2007, "An Experimental Investigation on the Emission Characteristics of HCCI Engine Operation Using n-Heptane," SAE Paper No. 2007-01-1854.
[25] Glassman, I., 1987, *Combustion*, Academic Press, New York.
[26] Peng, Z., Zhao, H., and Ladommatos, N., 2003, "Effect of Air/Fuel Ratios and EGR Rates on HCCI Combustion of n-Heptane, a Diesel Type Fuel," SAE Paper No. 2003-01-0747.
[27] Yelvington, P. E., Rallo, M. B., Liput, S., Tester, J. W., Green, W. H., and Yang, J., 2004, "Prediction of Performance Maps for Homogeneous-Charge Compression-Ignition Engines," Combust. Sci. Technol., **176**, pp. 1243–1282.
[28] Kongsereeparp, P. and Checkel, M. D., 2007, "Novel Method of Setting Initial Conditions for Multi-Zone HCCI Combustion Modeling," SAE Paper No. 2007-01-0674.
[29] Kongsereeparp, P. and Checkel, M. D., 2007, "Investigating the Effects of Reformed Fuel Blending in a Methane- or *n*-Heptane-HCCI Engine Using a Multi-Zone Model," SAE Paper No. 2007-01-0205.